© IWA Publishing 2020
1202

Water Practice & Technology Vol 15 No 4
doi: 10.2166/wpt.2020.091

Bio-adsorbent preparation based on Chinese Radix isatidis residue for Pb(II) removal

Yu-zhuo Shi, Xiao-chun Yin*, Guang-hui Si, Na-di Zhang, Mei-xia Du and Xin-hua Wang

School of Public Health, Gansu University of Chinese Medicine, Lanzhou 730000, China

*Corresponding author. E-mail: lzyxc@126.com

Abstract

A series of bio-adsorbents with potential for Pb(II) removal from wastewater were prepared by treating Radix isatidis residue (RIR) with integrated chemical treatment and fermentation methods. Batch experiments were used to test the adsorption and desorption performance of different bio-adsorbents. The results showed that treated RIRs had significantly enhanced adsorption capacity of 23.5 and 27.6 mg g^{-1} for Pb(II) within 50 minutes, in contrast to the raw RIR's 12.2 mg g^{-1}. RIR produced by modified chemical/fermentation treatment can remove up to 31.1 mg g^{-1}. After five adsorption/desorption cycles, about 75% of the adsorption capacities were maintained. This study is a novel approach to reusing the enormous quantity of Chinese herbal medicine residues.

Key words: absorbent, fermentation, modification, Pb(II), Radix isatidis residue (RIR), white-rot fungi

Highlights

- The bio-adsorbents for Pb(II) removal from wastewater were prepared by treating Radix isatidis residue with integrated chemical treatment and fermentation methods.
- The materials' morphology was determined, besides, batch experiments were used to test the adsorption and desorption performance of different bio-adsorbents.
- The adsorption capacities of the different adsorbents followed the order: D-RIR-NaOH-F > D-RIR-F > D-RIR-NaOH > D-RIR.
- The adsorption capacity of modified D-RIR remained above 75% of its initial level after five consecutive adsorption/desorption cycles.

INTRODUCTION

In recent decades, water pollution caused by heavy metals – for example, lead, cadmium, chromium and mercury – has become a serious problem because of their adverse effects on ecological systems and human health (Badruddoza *et al.* 2013a; Afkhami *et al.* 2010). The major concern with heavy metals is that most are highly toxic, carcinogenic and mutagenic at even relatively low concentrations (Ahmed *et al.* 2013; Badruddoza *et al.* 2013b). They are also non-biodegradable and tend to accumulate in organisms (Squadrone *et al.* 2016; Liu *et al.* 2018), making them indirectly harmful to human beings in some degree.

The treatment methods for heavy metal pollutants include adsorption, precipitation, nano-filtration, ion exchange, osmosis, etc (Jurado-Sánchez *et al.* 2015). Adsorption with various synthesized materials, such as activated carbon (Nowicki *et al.* 2015), carbon nanotubes (Ge *et al.* 2014; Yang *et al.* 2015), graphene (Nagarjuna *et al.* 2015) and metal-organic frameworks (MOFs) (Abney *et al.* 2014) has emerged as a promising wastewater treatment process. However, high cost and low reusability limit

Water Practice & Technology Vol 15 No 4
doi: 10.2166/wpt.2020.091

the widespread use of adsorbents in commercial applications (Yin *et al.* 2016). Conversely, natural polymer materials, including cellulose (Alatalo *et al.* 2015; Ganesan *et al.* 2016), rice husks (Vyas *et al.* 2013), wheat straw (Mahmood-Ul-Hassan *et al.* 2015), coconut shell (Huang *et al.* 2013), chitosan (Jiang *et al.* 2019), etc (Singh *et al.* 2018), have attracted increasing attention in heavy metal removal due to their extensive availability, eco-friendly nature and low cost (Thakur & Thakur 2015).

Cellulose is arguably the most abundant natural polymer and is the main component of plant fibres, giving plant their rigidity (Wei *et al.* 2014). Herb residue – for example, from Radix isatidis – is rich in cellulose and seen as a representative kind of concentrated natural resource, but also has pollution potential because it is highly susceptible to rot (Guo *et al.* 2013). In order to improve the potential utility of herb residues and protect the environment, various reutilisation studies have been done. Zhao & Zhou (2016) prepared a variety of bio-adsorbents to remove synthetic dyes from wastewater using an extraction residue of Salvia miltiorrhiza. Feng & Zhang (2013) used Chinese ephedra residue as a bio-adsorbent for Pb(II) removal from aqueous solutions. Li *et al.* (2010) extracted pine needle residues to adsorb methylene blue from aqueous solution. Although the researchers had taken advantage of the cellulose in herb residues to remove contaminants from wastewater, it is wrapped in lignin and is compact, resulting in low adsorption capacities and rates (Xue *et al.* 2018). Currently, physical, chemical and biological methods are commonly used to treat cellulose in natural polymer materials (Hokkanen *et al.* 2016; Anastopoulos *et al.* 2017; Yin *et al.* 2017).

In this study, chemical modification and fermentation treatment were used to prepare the bio-adsorbents to remove Pb(II) from wastewater. White-rot fungi, a common fermentation agent, can penetrate through lignin into the cell cavity and degrade the cellulose, hemicellulose and lignin by laccase, peroxidase and manganese peroxidise (Hildén *et al.* 2013; Kunjadia *et al.* 2016; Pamidipati & Ahmed 2017). Compared with physical and chemical methods, biological fermentation is ideal for wastewater treatment, because it causes no secondary pollution and saves energy (Yang *et al.* 2014; Yu & Choi 2018). In order to increase degradation efficiency, the cellulose structure was loosened with NaOH before fermentation. The Pb(II) adsorption and desorption properties of four bio-adsorbents were studied, providing a theoretical basis for the preparation of water bio-adsorbents on the basis of herb residue use.

MATERIALS AND METHODS

Materials

Fresh Radix isatidis residue (RIR) was obtained from a hospital affiliated to Gansu University of Chinese medicine (Gansu, China). White-rot fungi were obtained from China General Microbiological Culture Collection Center. Hydrochloric acid, sodium hydroxide, sodium carbonate, sulphuric acid and citric acid (all A.R. grade) came from Sinopharm Chemical Reagent Co. Ltd (Shanghai, China). Distilled water was produced by the laboratory's water purification system (Elix Reference, Merck Millipore, USA). All other reagents were of analytical grade, and all aqueous solutions were prepared with distilled water.

Preparation of bio-adsorbent

Herb residue

The herb's clean root slices were boiled three times with distilled water to remove all extracts. Subsequently, the extracted herb residue was treated with methanol (1:5, w/v) for removal of bioactive ingredients and pigments, this prevents them affecting the adsorption experiment. The solid residue,

Water Practice & Technology Vol 15 No 4
doi: 10.2166/wpt.2020.091

dried at 60 °C in an oven to constant weight, was ground after cooling to 0.5 to 1.0 mm size (referred to as D-RIR). The powders were stored in a desiccator until assay.

Chemical modification of herb residue

The D-RIR was put into a beaker with 1.0 mol L^{-1} NaOH (10:1, w/v), which was oscillated at constant temperature for 4 hours at 120 rpm. The solid residue was washed repeatedly with deionized water until neutral, and the product was dried to constant weight at 60 °C (referred to as D-RIR-NaOH).

Fermentation modification of herb residue

After sterilisation and cooling, white rot fungus was dispersed in liquid containing a known amount of D-RIR, sealed, placed in an incubator at 32 °C and rotated at 120 rpm for 9 days. The solid residue was dried at 60 °C (referred to as D-RIR-F).

Chemical/fermentation modification

The combined modification of the herb residue was conducted both chemically – NaOH – and by fermentation. The resulting adsorbent is referred to as D-RIR-NaOH-F.

Bio-adsorbent characterisation

The morphology of the materials' surfaces was observed using a scanning electron microscope (JSM, 5600LV, Japan), and the active functional groups were determined using a Perkin Elmer FTIR spectrometer (Thermo Fisher, USA).

Batch adsorption studies

25.0 mg of D-RIR-T (unified name of the four treated residues) was added to 25 mL of Pb(II) solution at different concentrations and vibrated at 30 °C and 120 rpm. The adsorption capacity (q_m) and removal rate (R) were determined using Equations (1) and (2).

$$q_m = (C_0 - C_e) \times V/m \quad (1)$$

$$R = (C_0 - C_e)/C_e \times 100\% \quad (2)$$

where C_0 and C_e are the concentrations of Pb(II) (mg L^{-1}) initially and after a known period of adsorption, respectively, V (L) the volume of aqueous solution, and m (g) the bio-adsorbent dosage. The adsorption capacity at different pH was investigated by adjusting the pH of the Pb(II) solution with 0.1 mol L^{-1} NaOH and HCL, and the adsorption kinetics were assessed by conducting the adsorption process for between 10 and 100 minutes. The main factors influencing adsorption were evaluated using the pseudo-first-order and second-order kinetic equations. The isothermal adsorption line of Pb(II) was tested in the solution concentration range from 10 to 100 mg L^{-1}. The Langmuir and Freundlich isothermal adsorption models were used to evaluate the main factors influencing the adsorption process.

Desorption and regeneration

When adsorption was complete, the adsorbent was separated and desorbed with 25 mL of HCl (0.5 mol L^{-1}) for 3 hours. The adsorbent was washed three times with deionized water until Pb(II)

Water Practice & Technology Vol 15 No 4
doi: 10.2166/wpt.2020.091

could not be detected in the eluent. Finally, the bio-adsorbent was dried and used in another adsorption cycle. The adsorption-desorption cycle was repeated five times and the desorption rate (D) calculated using Equation (3) (Sajab *et al.* 2013).

$$D\% = c_d/c_a \times 100\% \quad (3)$$

RESULTS AND DISCUSSION

Surface characterization

SEM analysis

The SEM images of RIR treated in different ways are shown in Figure 1. RIR modification produced significant changes. The original RIR surface was smooth, but after fermentation or alkali treatment, it was wrinkled. The surface was roughest when RIR was treated with alkali before fermentation, and there were many pores, due to destruction of the lignocellulose structure by the NaOH. Chemical/fermentation modification (Figure 1(d)) yielded particularly large numbers of micropores with structures favourable for heavy metal ion entry, which would enhance adsorption capacity.

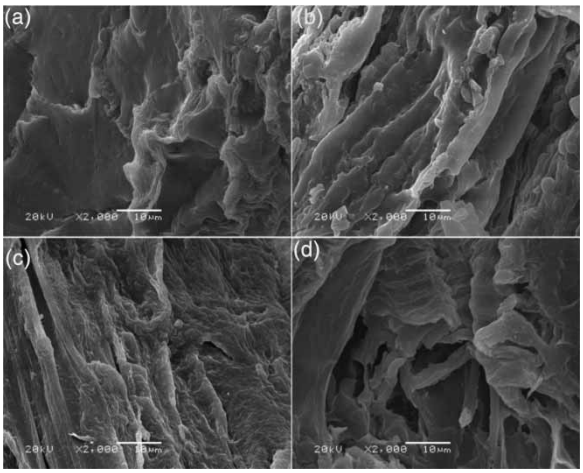

Figure 1 | The SEM images of D-RIR-Ts. (a:D-RIR; b:D-RIR-F; c:D-RIR-NaOH; d:D-RIR-NaOH-F).

Characteristic analysis

The FTIR spectroscopy provided information on the functional groups on the RIR surface before and after modification (Figure 2). D-RIR displayed several adsorption peaks at 3,390 to 3,396 cm^{-1} (OH stretching vibration in cellulose, hemicellulose and polysaccharide), 2,925 to 2,932 cm^{-1} (-CH_3 and -CH_2 vibration in cellulose), 1,649 cm^{-1} (water adsorbed in hemicellulose and cellulose), 1,031 cm^{-1} (Si-O stretching), 1,510 cm^{-1} (characteristic absorption peak of lignin).

After fermentation treatment, new peaks were observed at 1,239 cm^{-1}. The peaks of D-RIR-NaOH also changed significantly, indicating that alkali treatment removes lignin to a large extent. New peaks were also observed at 616 cm^{-1} in the FTIR spectra of D-RIR-NaOH-F, suggesting that these groups are the primary active adsorption sites.

Water Practice & Technology Vol 15 No 4
doi: 10.2166/wpt.2020.091

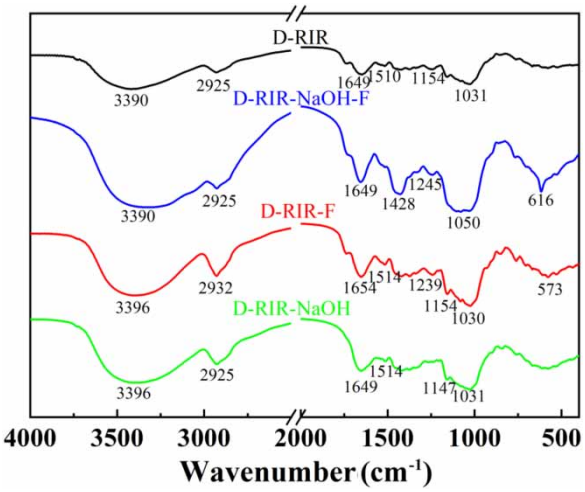

Figure 2 | FTIR spectra of the D-RIR-Ts before and after modification.

Removal of Pb(II) by D-RIR-Ts

Effect of pH

The pH of heavy metal ion solutions can affect the main metal ion species and the charge distribution on the bio-adsorbent surface (Al-Ghouti & Salih 2018; Dai *et al.* 2019), so adsorption capacity depends on solution pH to some extent. The adsorption capacities at different pH are shown in Figure 3. At low pH (<4), the adsorption capacity of the D-RIR-Ts increased rapidly with increasing pH. At pH 5 the adsorption capacity of D-RIR-NaOH-F reached 31.0 mg g^{-1}, about 1.5 times that of D-RIR-NaOH (23.21 mg g^{-1}), and 3 times that of D-RIR (11.9 mg g^{-1}). When pH is between 5 and 7, the adsorption capacities decreased slightly. This could be explained by the change of the surface-active sites – at low pH, the surface of bio-adsorbent was protonated, which reduced the number of binding sites that were available for uptake of metal ions in absorption. H^+ also competes with metal ions for adsorption sites, with increasing pH, the H^+ concentration gradually decreases, and the competition with metal ions weakens while adsorption capacity increases. At pH 5, the adsorption capacity of D-RIR-NaOH-F was highest, which might arise because pre-treatment with NaOH and fermentation led to greater adsorption capacity for Pb(II). With the addition of OH^- ions, the negative charges on the treated D-RIR surface increased correspondingly, producing more negative

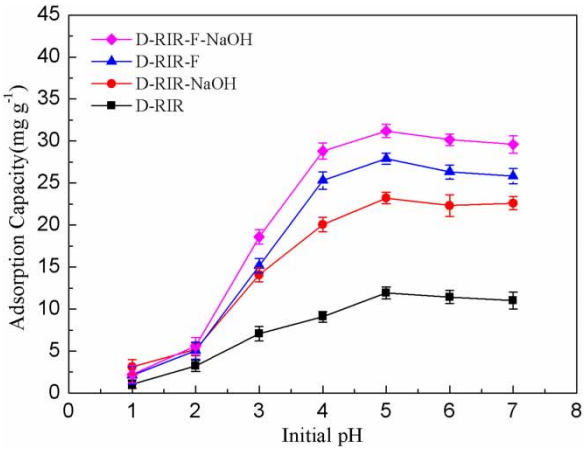

Figure 3 | Adsorption capacity of D-RIR-Ts at different pH.

Water Practice & Technology Vol 15 No 4
doi: 10.2166/wpt.2020.091

functional groups, and increasing the number of active groups that could participate in adsorption and thus improving adsorption capacity.

Effect of contact time

Figure 4 shows that there are two stages in the adsorption process: in the first 30 minutes adsorption is rapid, thereafter it is slower until equilibrium is reached. This could arise from the limited numbers of active binding sites on the bio-adsorbent surfaces (Abdel-Halim & Al-Deyab 2013). The adsorption capacity of D-RIR-NaOH-F was always the highest.

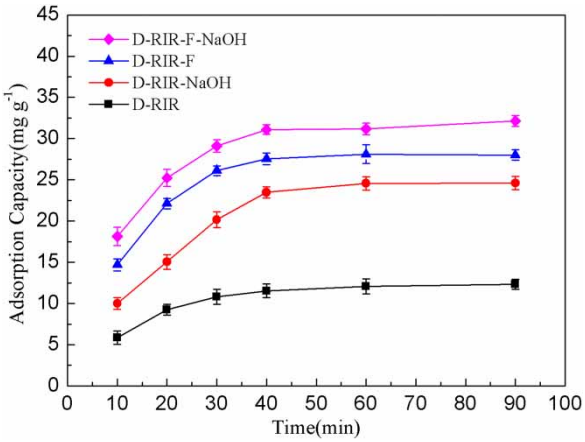

Figure 4 | Adsorption capacity of D-RIR-Ts at different time.

To improve understanding of the adsorption mechanism and evaluate the heavy metal ion adsorption capacity, the kinetics were studied using the pseudo-first- and second-order models expressed by Equations (4) and (5).

$$\log(q_e - q_t) = \log(q_e) - \left(\frac{k_1}{2.303}\right)t \tag{4}$$

$$\frac{t}{q_t} = \frac{1}{k_2 q_e^2} + \frac{t}{q_e} \tag{5}$$

where q_t and q_e represent Pb(II) adsorption by bio-adsorbents (mg g^{-1}), and k_1 (min^{-1}) and k_2 (g mg^{-1} min) are the rate constants for the models. Data fitting results are shown in Table 1.

Table 1 | Pseudo-first-order and pseudo-second-order parameters

		Pseudo-first-order model				Pseudo-second-order model		
		$q_{e,exp}$ (mg g^{-1})	$q_{e,cal}$ (mg g^{-1})	k_1 (min^{-1})	R_1^2	$q_{e,cal}$ (mg g^{-1})	k_2 (g mg^{-1} min)	R_2^2
Pb(II)	D-RIR	12.40	13.70	4.38×10^{-2}	0.992	7.575	1.23×10^{-2}	0.956
	D-RIR-F	24.70	46.98	6.41×10^{-2}	0.975	30.25	1.69×10^{-2}	0.994
	D-RIR-NaOH	22.60	35.6	8.52×10^{-2}	0.932	27.07	2.48×10^{-2}	0.990
	D-RIR-NaOH-F	32.10	45.4	11.51×10^{-1}	0.914	35.71	3.98×10^{-3}	0.995

The pseudo-first-order model's calculated value for D-RIR (12.4 mg g^{-1}) was closer to the experimental value (13.7 mg g^{-1}) than that from the pseudo-second-order model. Moreover, the correlation coefficient (R_1^2) was higher than R_2^2, indicating that adsorption was described better by

Water Practice & Technology Vol 15 No 4
doi: 10.2166/wpt.2020.091

the pseudo-first-order model. This, in turn, indicated that Pb(II) adsorption of D-RIR is a physical process. However, the correlation coefficients (R_2^2) of D-RIR-F, D-RIR-NaOH, D-RIR-NaOH-F of the pseudo-second-order kinetic model all exceeded 0.99, and the calculated adsorption capacities were closer to the experimental data, indicating that their Pb(II) adsorption was chemical.

Effect of initial concentration

The initial concentration of metal ions has a significant influence on bio-adsorbent performance. To investigate this in relation to Pb(II) with respect to D-RIR-Ts, initial Pb(II) concentrations were adjusted in the range 10–100 mg L^{-1}. As can be seen in Figure 5, adsorption capacity increased gradually with increasing initial Pb(II) concentration. The increase in metal ion concentration provides an adsorption driving force for bio-adsorbents (Liu *et al.* 2010). When the initial concentration was increased further, the active adsorption sites tended to become saturated. The removal capacity of Pb(II) decreased in the order D-RIR-NaOH-F >D-RIR-F >D-RIR-NaOH > D-RIR, possibly due to the formation of an extracellular mucus sheath connecting mycelia and biomass, which enables the fungi to degrade lignin and hemicellulose, to expose the active groups of cellulose and increase the adsorption capacity of cellulose to metal ions (Mäkelä *et al.* 2013; Waliszewska *et al.* 2019).

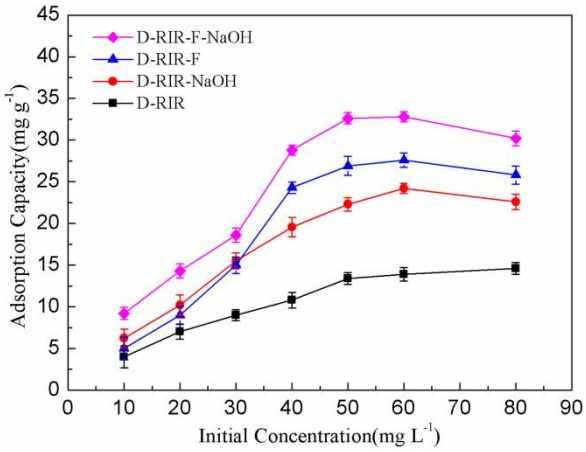

Figure 5 | Adsorption capacity of D-RIR-Ts at different initial concentrations.

Attempts were made to model the equilibrium data using the linear forms of the Langmuir and Freundlich models, expressed, respectively, in Equations (6) and (7).

$$\frac{c_e}{q_e} = \frac{c_e}{Q_m} + \frac{1}{Q_m K_L}. \tag{6}$$

$$\log q_e - \log K_F + \frac{1}{n} \times \log C_e \tag{7}$$

where q_e (mg g^{-1}) is the Pb(II) uptake capacity and Q_m (mg g^{-1}) the theoretical maximal adsorption capacity, C_e (mg L^{-1}) the equilibrium concentration of Pb(II), K_L (L mg^{-1}) and K_F (mg^{1-n} g^{-1} L^{-n}) the isothermal constants of the Langmuir and Freundlich isothermal equations, respectively, and n the constant describing the adsorption strength.

Two isothermal models were used to fit the experimental data – see Table 2. The Langmuir correlation coefficient, R_L^2 (>0.99), for D-RIR-NaOH-F, D-RIR-F and D-RIR-NaOH were higher than the Freundlich correlation coefficients, R_F^2, and the calculated values using the Langmuir equation were closer to the experimental values. On this basis it could be concluded that the adsorption

Water Practice & Technology Vol 15 No 4
doi: 10.2166/wpt.2020.091

Table 2 | Isotherm parameters for the Langmuir and Freundlich isotherm models

			Langmuir model			Freundlich model		
		$q_{e,exp}$ (mg g^{-1})	$q_{e,cal}$ (mg g^{-1})	K_L (L mg^{-1})	R_L^2	K_F (mg^{1-n} g^{-1} L^{-n})	n	R_F^2
Pb(II)	D-RIR	14.60	20.00	3.72×10^{-2}	0.987	1.197	1.550	0.992
	D-RIR-F	27.60	30.30	1.55×10^{-1}	0.991	7.886	3.039	0.961
	D-RIR-NaOH	23.80	25.78	1.12×10^{-1}	0.990	3.098	1.206	0.985
	D-RIR-NaOH-F	32.50	33.30	1.138	0.990	5.767	2.101	0.854

process was fitted better by the Langmuir isothermal model, indicating that Pb(II) adsorption in this case was a single-layer chemisorption process. However, the Freundlich correlation coefficient, R_F^2, was close to 1 for D-RIR, and there was little difference between the calculated and experimental values, suggesting that the Freundlich isothermal model provides a better description of D-RIR adsorption.

Table 3 is a comparison of q_{max} for Pb(II) obtained in this study with bio-adsorbents used in other work. The adsorption capacity of D-RIR-NaOH-F exceeds that of some other bio-adsorbents.

Table 3 | Comparison of Pb(II) adsorption for various bio-adsorbents

Bio-adsorbent	q_{max} (mg g^{-1})	Reference
Coffee residues	9.91	Wu *et al.* (2015)
Egg shells	22.80	Ahmad *et al.* (2012)
Coffee husks	37.04	Alhogbi (2017)
Carnauba tree	28.00	Oliveira *et al.* (2020)
Lignocellulosic-NaOH	134.41	Wang *et al.* (2018)
Zygophyllum coccineum	25.50	Amro (2019)
D-RIR-NaOH-F	30.60	this study
Agaricus bisporus-NaOH	86.40	Long *et al.* (2014)

Desorption and regeneration

D-RIR-NaOH-F, the best bio-adsorbent for Pb(II) in this work, was used to study adsorption and desorption conditions. Its reusability for Pb(II) adsorption is shown in Figure 6. After five consecutive

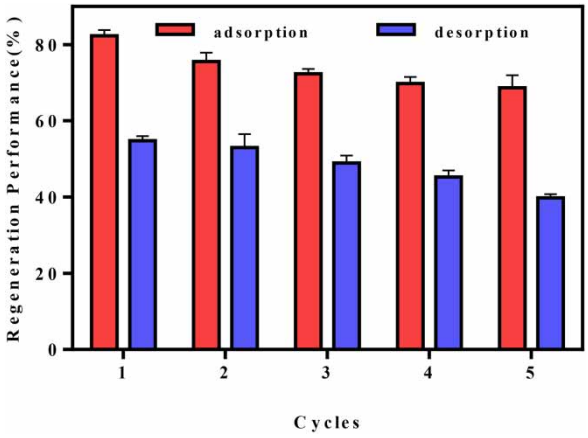

Figure 6 | Five cycle regeneration performance of D-RIR-NaOH-F for Pb(II).

Water Practice & Technology Vol 15 No 4
doi: 10.2166/wpt.2020.091

adsorption/desorption cycles, the adsorption rate was still 75% of the original level and only about 10% lower than after its first regeneration. In addition, the desorption rate of HCl was as high as 50% (Sajab *et al.* 2013). In other words, the recycling performance of D-RIR-NaOH-F is promising.

CONCLUSIONS

The bio-adsorbents based on Radix Isatidis residues to remove Pb(II) from wastewater were prepared using two modification methods. The adsorption capacities of the different adsorbents followed the order: D-RIR-NaOH-F >D-RIR-F >D-RIR-NaOH >D-RIR. The highest capacity was achieved by D-RIR-NaOH-F, at about 31.1 mg g^{-1} in 50 minutes. The adsorption capacity of modified D-RIR remained above 75% of its initial level after five consecutive adsorption/desorption cycles. Not only can D-RIR-NaOH-F be used to remove Pb(II) from wastewater, it is also a means of reusing a common natural waste material.

ACKNOWLEDGEMENTS

This work was supported by Natural Science Foundation of Gansu Science and Technology Department (17JR5RA170) and the Foundation of Gansu Educational Committee of China (2018A-047).

DATA AVAILABILITY STATEMENT

All relevant data are included in the paper or its Supplementary Information.

REFERENCES

Abdel-Halim, E. S. & Al-Deyab, S. S. 2013 Preparation of poly(acrylic acid)/starch hydrogel and its application for cadmium ion removal from aqueous solutions. *Reactive and Functional Polymers* **75**(1), 1–8. doi:10.1016/j.reactfunctpolym.2013.12.003.

Abney, C. W., Gilhula, J. C., Lu, K. & Lin, W. 2014 Metal-organic framework templated inorganic sorbents for rapid and efficient extraction of heavy metals. *Advanced Materials* **26**(47), 7993–7997. doi:10.1002/adma.201403428.

Afkhami, A., Saber-Tehrani, M. & Bagheri, H. 2010 Modified maghemite nanoparticles as an efficient adsorbent for removing some cationic dyes from aqueous solution. *Desalination* **263**(1–3), 240–248. doi:10.1016/j.desal.2010.06.065.

Ahmad, M., Usman, A. R. A., Lee, S. S., Kim, S. C., Joo, J. H., Yang, J. E. & Ok, Y. S. 2012 Eggshell and coral wastes as low cost sorbents for the removal of Pb^{2+}, Cd^{2+} and Cu^{2+} from aqueous solutions. *Journal of Industrial & Engineering Chemistry* **18**(1), 198–204. doi:10.1016/j.jiec.2011.11.013.

Ahmed, M. A., Ali, S. M., El-Dek, S. I. & Galal, A. 2013 Magnetite-hematite nanoparticles prepared by green methods for heavy metal ions removal from water. *Materials Science and Engineering B* **178**(10), 744–751. doi:10.1016/j.mseb.2013.03.011.

Alatalo, S. M., Pileidis, F. D., Mäkilä, E., Marta, S., Repo, E., Salonen, J., Sillanpää, M. & Titirici, M. M. 2015 Versatile cellulose-based carbon aerogel for the removal of both cationic and anionic metal contaminants from water. *ACS Applied Materials Interfaces* **7**(46), 25875–25883. doi: 10.1021/acsami.5b08287.

Al-Ghouti, M. A. & Salih, N. R. 2018 Application of eggshell wastes for boron remediation from water. *Journal of Molecular Liquids* **256**, 599–610. doi:10.1016/j.molliq.2018.02.074.

Alhogbi, B. G. 2017 Potential of coffee husk biomass waste for the adsorption of Pb(II) ion from aqueous solutions. *Sustainable Chem Pharm* **6**, 21–25. doi:10.1016/j.scp.2017.06.004.

Amro, A. N. 2019 Removal of lead and copper ions from water using powdered Zygophyllum coccineum biomass. *International Journal of Phytoremediation* **21**(4), 1457–1462. doi:10.1080/15226514.2019.1633267.

Anastopoulos, I., Karamesouti, M., Mitropoulos, A. C. & Kyzas, G. Z. 2017 A review for coffee adsorbents. *Journal of Molecular Liquids* **229**, 555–565. doi:10.1016/j.molliq.2016.12.096.

Badruddoza, A. Z., Shawon, Z. B., Tay, W. J., Hidajat, K. & Uddin, M. S. 2013a Fe_3O_4/cyclodextrin polymer nanocomposites for selective heavy metals removal from industrial wastewater. *Carbohydr Polym* **91**(1), 322–332. doi:10.1016/j.carbpol.2012.08.030.

Water Practice & Technology Vol 15 No 4
doi: 10.2166/wpt.2020.091

Badruddoza, A. Z., Shawon, Z. B., Rahman, M. T., Hao, K. W., Hidajat, K. & Uddin, M. S. 2013b Ionically modified magnetic nanomaterials for arsenic and chromium removal from water. *Chemical Engineering Journal* **225**(Complete), 607–615. doi:10.1016/j.cej.2013.03.114.

Dai, Y., Zhang, K., Meng, X., Li, J., Guan, X., Sun, Q., Sun, Y. & Wang, W. 2019 New use for spent coffee ground as an adsorbent for tetracycline removal in water. *Chemosphere* **215**(JAN), 163–172. doi:10.1016/j.chemosphere.2018.09.150.

Feng, N. & Zhang, F. 2013 Untreated Chinese ephedra residue as biosorbents for the removal of Pb_2^+ ions from aqueous solutions. *Procedia Environmental Sciences* **18**(Complete), 794–799. doi:10.1016/j.proenv.2013.04.107.

Ganesan, K., Dennstedt, A., Barowski, A. & Ratke, L. 2016 Design of aerogels, cryogels and xerogels of cellulose with hierarchical porous structures. *Materials & Design* **92**(15), 345–355. doi:10.1016/j.matdes.2015.12.041.

Ge, Y., Li, Z., Xiao, D., Xiong, P. & Ye, N. 2014 Sulfonated multi-walled carbon nanotubes for the removal of copper (II) from aqueous solutions. *Journal of Industrial and Engineering Chemistry* **20**(4), 1765–1771. doi:10.1016/j.jiec.2013.08.030.

Guo, F., Dong, Y., Dong, L. & Jing, Y. Z. 2013 An innovative example of herb residues recycling by gasification in a fluidized bed. *Waste Management* **33**(4), 825–832. doi:10.1016/j.wasman.2012.12.009.

Hildén, K., Mäkelä, M. R., Lundell, T., Kuuskeri, J., Chernykh, A., Golovleva, L., Archer, D. B. & Hatakka, A. 2013 Heterologous expression and structural characterization of two low pH laccases from a biopulping white-rot fungus physisporinus rivulosus. *Applied Microbiology and Biotechnology* **97**(4), 1589–1599. doi:10.1007/s00253-012-4011-6.

Hokkanen, S., Bhatnagar, A. & Sillanpää, M. 2016 A review on modification methods to cellulose-based adsorbents to improve adsorption capacity. *Water Research* **91**(15), 156–173. doi:10.1016/j.watres.2016.01.008.

Huang, R., Wen, Y. H., Shao, G. F. & Sun, S. G. 2013 Insight into the melting behavior of Au–Pt core–Shell nanoparticles from atomistic simulations. *The Journal of Physical Chemistry C* **117**(8), 4278–4286. doi:10.1021/jp312048 k.

Jiang, X. C., Xiang, X. T., Peng, S. J. & Hou, L. X. 2019 Facile preparation of nitrogen-doped activated mesoporous carbon aerogel from chitosan for methyl orange adsorption from aqueous solution. *Cellulose* **26**(2), 4512–4527. doi:10.1007/s10570-019-02368-2.

Jurado-Sánchez, B., Sattayasamitsathit, S., Gao, W., Santos, L., Fedorak, Y., Singh, V. V., Orozco, J., Galarnyk, M. & Wang, J. 2015 Self-propelled activated carbon janus micromotors for efficient water purification. *Small* **11**(4), 499–506. doi:10.1002/smll.201402215.

Kunjadia, P. D., Sanghvi, G. V., Kunjadia, A. P., Mukhopadhyay, P. N. & Dave, G. S. 2016 Role of ligninolytic enzymes of white rot fungi (Pleurotus spp.) grown with azo dyes. *Springer Plus* **5**(1), 1487. doi:10.1186/s40064-016-3156-7.

Li, H. P., Han, X. L. & Liu, G. J. 2010 Study on the adsorption performance of adsorbing methylene blue from its aqueous solution by extraction residues of pine needles extracted in GXLs. *Journal of Chemical Engineering of Chinese Universities* **24**(6), 1059–1064. doi:10.1631/jzus.A1000244.

Liu, Y., Wang, W. & Wang, A. 2010 Adsorption of lead ions from aqueous solution by using carboxymethyl cellulose-g-poly (acrylic acid)/attapulgite hydrogel composites. *Desalination* **259**(1–3), 258–264. doi:10.1016/j.desal.2010.03.039.

Liu, S., Duan, Z., He, C. & Xu, X. 2018 Rapid removal of Pb^{2+} from aqueous solution by phosphate-modified baker's yeast. *RSC Advances* **8**(15), 8026–8038. doi:10.1039/C7RA13545A.

Long, Y., Lei, D., Ni, J., Ren, Z., Chen, C. & Xu, H. 2014 Packed bed column studies on lead(II) removal from industrial wastewater by modified agaricus bisporus. *Bioresource Technology* **152**, 457–463. doi:10.1016/j.biortech.2013.11.039.

Mahmood-Ul-Hassan, M., Suthar, V., Rafique, E., Ahmad, R. & Yasin, M. 2015 Kinetics of cadmium, chromium, and lead sorption onto chemically modified sugarcane bagasse and wheat straw. *Environmental Monitoring and Assessment* **187**(7), 470. doi:10.1007/s10661-015-4692-2.

Mäkelä, M. R., Lundell, T., Hatakka, A. & Hildénet, K. 2013 Effect of copper, nutrient nitrogen, and wood-supplement on the production of lignin-modifying enzymes by the white-rot fungus Phlebia radiata. *Fungal Biology* **117**(1), 62–70. doi:10.1016/j.funbio.2012.11.006.

Nagarjuna, R., Challagulla, S., Alla, N., Ganesan, R. & Roy, S. 2015 Synthesis and characterization of reduced-graphene oxide/TiO_2/Zeolite-4A: a bifunctional nanocomposite for abatement of methylene blue. *Materials Design* **86**(5), 621–626. doi:10.1016/j.matdes.2015.07.116.

Nowicki, P., Kazmierczak, J. & Pietrzak, R. 2015 Comparison of physicochemical and sorption properties of activated carbons prepared by physical and chemical activation of cherry stones. *Powder Technology* **269**, 312–319. doi:10.1016/j.powtec.2014.09.023.

Oliveira, M. R. F., Abreu, K. D. V., Romão, A. L. E., Davi, D. M. B., Magalhães, C. E. D. C. & Alves, C. R. 2020 Carnauba (Copernicia prunifera) palm tree biomass as adsorbent for Pb(II) and Cd(II) from water medium. *Environmental Science and Pollution Research* **15**, 1–12. doi:10.1007/s11356-020-07635-5.

Pamidipati, S. & Ahmed, A. 2017 Degradation of lignin in agricultural residues by locally isolated fungus *Neurospora discreta*. *Applied Biochemistry and Biotechnology* **181**(4), 1561–1572. doi:10.1007/s12010-016-2302-6.

Sajab, M. S., Chia, C. H., Zakaria, S. & Khiew, P. S. 2013 Cationic and anionic modifications of oil palm empty fruit bunch fibers for the removal of dyes from aqueous solutions. *Bioresource Technology* **128**(Complete), 571–577. doi:10.1016/j.biortech.2012.11.010.

Singh, N. B., Nagpal, G., Agrawal, S. & Rachna 2018 Water purification by using adsorbents: a review. *Environment Technology Innovation* **11**, 187–240. doi:10.1016/j.eti.2018.05.006.

Squadrone, S., Brizio, P., Stella, C., Prearo, M., Pastorino, P., Serracca, L., Ercolini, C. & Abete, M. C. 2016 Presence of trace metals in aquaculture marine ecosystems of the northwestern Mediterranean Sea (Italy). *Environmental Pollution* **215**, 77–83. doi:10.1016/j.envpol.2016.04.096.

Water Practice & Technology Vol 15 No 4
doi: 10.2166/wpt.2020.091

Thakur, V. K. & Thakur, M. K. 2015 Recent advances in green hydrogels from lignin: a review. *International Journal of Biological Macromolecules* **72**, 834–847. doi:10.1016/j.ijbiomac.2014.09.044.

Vyas, A. H., Jauhari, S. & Murthy, Z. V. P. 2013 Chemically modified rice husk adsorbents, characterization and removal of palladium(II) from aqueous solutions. *Journal of Dispersion Science and Technology* **34**(3), 369–380. doi:10.1080/01932691.2012.667719.

Waliszewska, B., Mirosław, M., Zborowska, M., Goliński, P., Rutkowski, P. & Szentner, K. 2019 Changes in the chemical composition and the structure of cellulose and lignin in elm wood exposed to various forms of arsenic. *Cellulose* **2019**(26), 6303–6315. doi:10.1007/s10570-019-02511-z.

Wang, C., Wang, H. & Gu, G. 2018 Ultrasound-assisted xanthation of cellulose from lignocellulosic biomass optimized by response surface methodology for Pb(II) sorption. *Carbohydrate Polymers* **182**, 21–28. doi:10.1016/j.carbpol.2017.11.004.

Wei, Y., Shimanouchi, T., Wu, S. & Kimura, Y. 2014 Investigation of the degradation kinetic parameters and structure changes of microcrystalline cellulose in subcritical water. *Energy Fuels* **28**(11), 6974–6980. doi:10.1021/ef501702q.

Wu, C. H., Kuo, C. Y. & Guan, S. S. 2015 Adsorption kinetics of lead and zinc ions by coffee residues. *Polish Journal of Environmental Studies* **24**, 761–767. doi:10.15244/pjoes/31222.

Xue, Y. T., Du, C. F., Wu, Z. S. & Zhang, L. H. 2018 Relationship of the cellulose and lignin contents in biomass to the structure and RB-19 adsorption behavior on activated carbon. *New Journal of Chemistry* **42**, 16493–16502. doi:10.1039/C8NJ03007C.

Yang, P. F., Sanno, M., Ganse, B., Koy, T., Brüggemann, G. P., Müller, L. P. & Rittweger, J. 2014 In vivo application of an optical segment tracking approach for bone loading regimes recording in humans: a reliability study. *Medical Engineering & Physics* **36**(8), 1041–1046. doi:10.1016/j.medengphy.2014.05.005.

Yang, S., Kim, H., Narayanan, S., Mckay, L. S. & Wang, E. N. 2015 Dimensionality effects of carbon-based thermal additives for microporous adsorbents. *Materials & Design* **85**, 520–526. doi:10.1016/j.matdes.2015.06.166.

Yin, X. C., Liu, X., Fan, J. C., Wu, J. J., Men, J. L. & Zheng, G. S. 2016 Preparation of gel resins and removal of copper and lead from water. *Journal of Applied Polymer Science* **134**(7), 44466. doi:10.1002/app.44466.

Yin, X. C., Wu, J. J., Zhao, Y. & Lin, X. 2017 Preparation of polymer modified xanthan gum/hydroxyapatite composite hydrogel and its absorption for metal ions. *Acta Scientiae Circumstantiae* **37**(2), 633–641. doi:10.13671/j.hjkxxb.2016.0180.

Yu, S. W. & Choi, H. J. 2018 Application of hybrid bead, persimmon leaf and chitosan for the treatment of aqueous solution contaminated with toxic heavy metal ions. *Water Science and Technology* **78**(4), 837–847. doi:10.2166/wst.2018.354.

Zhao, S. & Zhou, T. 2016 Biosorption of methylene blue from wastewater by an extraction residue of Salvia miltiorrhiza Bge. *Bioresource Technology* **219**, 330–337. doi:10.1016/j.biortech.2016.07.121.